A MESHFREE THREE-DIMENSIONAL (3-D) NUMERICAL MODEL TO STUDY TRANSPORT PHENOMENA IN SINGLE PLANT CELLS DURING DRYING

C.M. Rathnayaka Mudiyanselage *[1, 2], H.C.P. Karunasena [3], Y.T. Gu [1], L. Guan [1], J. Banks [1] & W. Senadeera [1]

[1] *Queensland University of Technology (QUT), Science and Engineering Faculty, School of Chemistry Physics and Mechanical Engineering.*

[2] *Department of Chemical and Process Engineering, Faculty of Engineering, University of Moratuwa, Moratuwa, Sri Lanka.*

[3] *Department of Mechanical and Manufacturing Engineering, Faculty of Engineering, University of Ruhuna, Hapugala, Galle, Sri Lanka.*

[a] charith.rathnayaka@hdr.qut.edu.au, [b]chaminda@mme.ruh.ac.lk, [c]yuantong.gu@qut.edu.au, [d]l.guan@qut.edu.au, [e]j.banks@qut.edu.au, [f]w3.senadeera@qut.edu.au

* Corresponding Author

Keywords: Food drying; Meshfree methods; Plant cell modelling; Smoothed Particle Hydrodynamics (SPH); Three-dimensional (3-D) model; Mass transfer

Abstract. To improve the performance of food drying operations, an in depth understanding of the related transport phenomena in plant food cellular structures is necessary. A three-dimensional (3-D) numerical model has been developed to investigate the morphological changes and related solid and fluid transfer mechanisms of single parenchyma cells of apple during drying. This numerical model was developed by coupling a meshfree particle based method: Smoothed Particle Hydrodynamics (SPH) with a Discrete Element Method (DEM). Compared to conventional grid-based numerical modelling techniques: Finite Element Methods (FEM) and Finite Difference Methods (FDM), the proposed meshfree model can better predict the deformations and cellular shrinkage within a wide range of moisture content. The model contains two main components: cell fluid and cell wall. The cell fluid model is based on SPH and represents the cell protoplasm as a homogeneous Newtonian liquid. The cell wall model is based on DEM and approximates the cell wall as an incompressible Neo-Hookean solid. The sensitivity and the consistency of the model towards mass transfer parameters of the system have been studied via simulating the cell inflation under different conditions.

Introduction

Drying is one of the most common and cost effective methods for increasing the shelf life of plant foods and for the production of traditional as well as novel processed products [1]. It is employed to preserve approximately one fifth (1/5) of the planet's perishable crops [2]. During drying, the moisture content of fruits and vegetables are brought down in order to decelerate the biological activities present. With the removal of water, the food cellular structure undergoes structural deformations which influence drying operational performance, dried food quality and the final market value. Therefore, to develop effective and efficient food drying operations, it is important that these cellular structural deformations are maintained under favourable limits. In order to optimise the cellular structural deformations, it is crucial to have a comprehensive understanding of the underlying transport phenomena. The key driving forces of related transport phenomena are moisture content [3-6] and the drying temperature . In such a system, moisture content has a strong relationship with the cell turgor pressure[7] and similarly, drying temperature has a relationship with relative humidity. To derive the most appropriate relationship among such driving forces, cellular morphogenesis and underlying transport phenomena; various microscale theoretical [8] and empirical [3, 4, 9] models have been developed.

Numerical modelling has been utilised as an efficient tool in studies of deformational analysis of various materials. Until the recent times this had not been used for comprehensively analysing micro-structural deformations of food materials during drying. However recently, numerical modelling has attracted increased attention as a viable tool for serving this purpose [10]. It is believed that through an accomplished numerical drying model, immense benefits could be achieved in food drying engineering in terms of drying process performance and product quality through optimising related mass transfer phenomena and deformational characteristics. In this study, a three-dimensional (3-D) numerical model has been developed to better investigate the morphological changes and related solid and fluid dynamics of a single apple parenchyma cell, during drying. To implement the model, more versatile and novel meshfree particle methods have been chosen over classical grid based methods. Furthermore, the sensitivity and the consistency of the model towards mass transfer parameters of the system have been studied.

Methodology

3-D Representation of the Cell. For this study, it should be noted that a single cell of a parenchyma tissue is considered, which is the main building block of most plant structures. This type of a cell could be mechanically regarded as a stiff, thin-walled vessel surrounding a viscous fluid. Correspondingly, the developed numerical model is composed of two main model components: cell wall and cell fluid. Based on the literature, the basic geometrical shape of a single cell was assumed to be spherical (see Fig. 1) [11]. In the cell fluid model, the fluid volume was approximated to a sphere and the cell wall was approximated to a hollow 3-D spherical shell. The cell fluid hydrodynamic pressure was balanced by the cell wall tension. The whole system was considered to be incompressible and isothermal. After establishing the fundamental approximations, cell fluid and cell wall were then separately discretised into particle domains. The intention of this discretisation is to represent the whole system using a set of non-interconnected particles according to the fundamentals of Meshfree Particle Methods (e.g. Smoothed Particle Hydrodynamics (SPH) [12]). Due to the flexibility of the particle framework used in this model, it could be easily scaled up to multiple cell systems by aggregating more individual cells [13, 14]. This particular modelling technique also ensures the ability to describe the mechanisms in the subcellular structure.

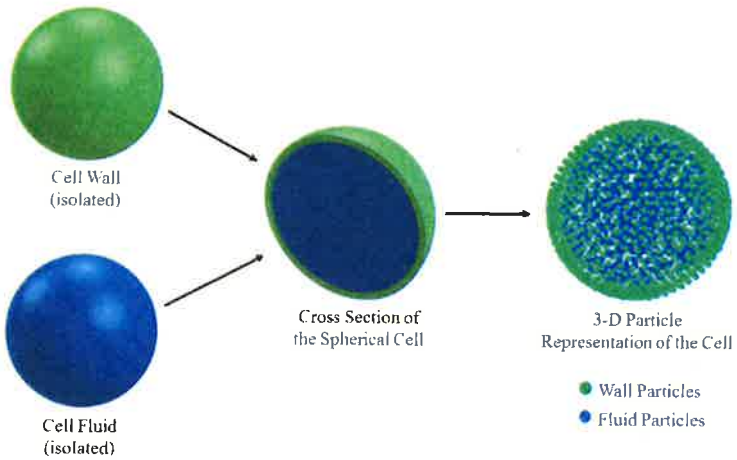

Fig. 1. 3-D representation of the cell model, which is composed of two sub-models: cell fluid model and cell wall model

Cell Fluid Model. By considering the large water content present in the cell protoplasm, which can be about 80-90% by volume [15], the cell fluid was approximated to a homogeneous Newtonian fluid equivalent to water, but with an elevated viscosity. This was then modelled with Smoothed Particle Hydrodynamics (SPH) considering low Reynolds number flow characteristics [13, 15]. In order to model the physical characteristics present in cell fluid, four different types of forces

were used: pressure forces ($\boldsymbol{F^p}$), viscous forces ($\boldsymbol{F^v}$), wall-fluid repulsion forces ($\boldsymbol{F^{rw}}$) and wall-fluid attraction forces ($\boldsymbol{F^a}$) as presented in Fig. 2 [10]. The combined effect of these forces was used to define the total force $\boldsymbol{F_i}$ on a given fluid particle i as,

$$\boldsymbol{F_i} = \boldsymbol{F^p_{ii'}} + \boldsymbol{F^v_{ii'}} + \boldsymbol{F^{rw}_{ik}} + \boldsymbol{F^a_{ik}}\,. \tag{1}$$

where i' represents the neighbouring fluid particles and k stand for the interacting wall particles

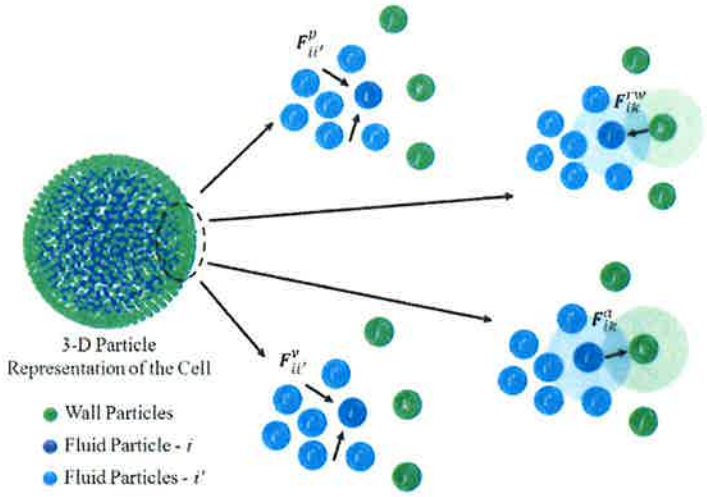

Fig. 2. Force fields on the 3-D fluid particle domain: pressure forces ($\mathbf{F^p}$), viscous forces ($\mathbf{F^v}$), wall-fluid repulsion forces ($\mathbf{F^{rw}}$) and wall-fluid attraction forces ($\mathbf{F^a}$)

Cell Wall Model. The cell wall was approximated to a Neo-Hookean solid material. It was treated as a particle scheme composed of interconnected discrete elements connected to each other as a network. Each element carried properties of the corresponding cell wall element. Physical behaviour of the wall and the corresponding deformations were represented by the displacement of respective particles using four types of force interactions : stiff forces ($\boldsymbol{F^e}$), damping forces ($\boldsymbol{F^d}$), wall-fluid repulsion forces ($\boldsymbol{F^{rf}}$) and wall-fluid attraction forces ($\boldsymbol{F^a}$), as illustrated in Fig. 3 [10]. Accordingly, the total force ($\boldsymbol{F_k}$) on any wall particle k was derived as,

$$\boldsymbol{F_k} = \boldsymbol{F^e_{kj}} + \boldsymbol{F^d_{kj}} + \boldsymbol{F^{rf}_{ki}} + \boldsymbol{F^a_{ki}}\,, \tag{2}$$

where, for each wall particle k, i depict the neighbouring fluid particles, j bonded wall particles and l non-bonded wall particles

Analysis. The previously mentioned model features and interactions were numerically set up with the physical properties of a representative apple cell having properties as given in Table 1. The software tool, COMSOL Multiphysics (COMSOL) was used to generate the initial 3-D particle arrangements in 3-D spherical geometries corresponding to both the cell fluid and cell wall. There is the possibility to define and fine-tune the initial particle gap and the cell geometrical characteristics using COMSOL in order to obtain the initial particle positions with the preferred particle resolution. The fluid particle scheme was placed without any interconnections among particles, adhering to the SPH fundamentals. In the cell wall, spring networks joining the cell wall particles were used according to the DEM fundamentals [10, 14].

As the model evolves with time according to the difference between the cell turgor pressure and the osmotic potential, the mass of the cell fluid tends to change and this leads to slight density variations [10]. Such changes of density cause significant changes in cell turgor pressure. These are governed by an equation of state (EOS) and such turgor pressure variations push the cell wall inwards

(shrinkage) or outwards (inflation) causing the cell volume, equivalent diameter and surface area to change. Based on such cell volume changes, the cell turgor pressure varies since it has to be counterbalanced by the cell wall tension. The changes in cell turgor pressure leads to the cell fluid mass increments (governed by a mass transfer equation) or losses [10]. This is repeats as a cycle until the system reaches steady state. The mass transfer characteristics of the system have a significant influence on the behaviour of the developed model. The accuracy of the model predictions and the stability of the simulations depend on the selected mass transfer parameters. For example, the cell wall hydrodynamic conductivity (or the cell wall permeability-L_P) could be given as a parameter. To study the sensitivity of the model towards the L_P magnitude, the simulations were run with a range of L_P and the behaviour of the model and its predictions were observed.

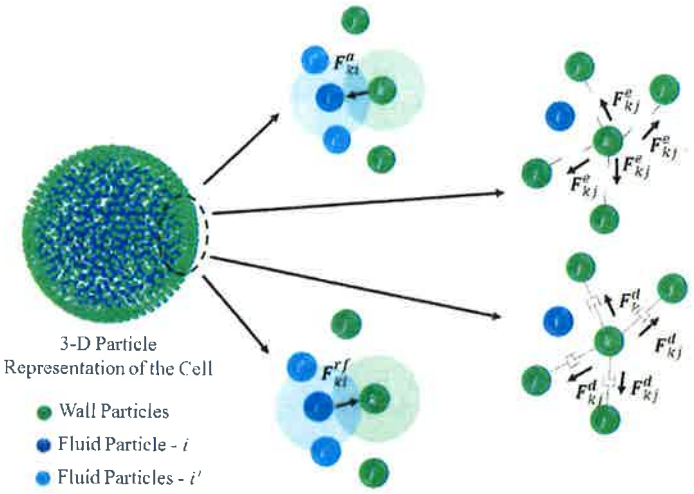

Fig. 3. Force fields on the 3-D wall particle domain: stiff forces ($\mathbf{F}^{e}$), damping forces ($\mathbf{F}^{d}$), wall-fluid repulsion forces ($\mathbf{F}^{rf}$) and wall-fluid attraction forces ($\mathbf{F}^{a}$)

Table 1: Values of the physical parameters adopted in the cell model

Parameter	Value	Reference
Initial cell radius	75 $[\mu m]$	[5]
Cell wall shear modulus (G)	18 $[MPa]$	[16]
Initial thickness of the cell wall (t)	126 $[nm]$	[17]
Cell wall damping ratio (γ)	5×10^{-6} $[Nm^{-1}s]$	Set([10])
Cell fluid viscosity (μ)	0.1 $[Pas]$	Set ([14, 15])
SPH smoothing length (h)	12.2 $[\mu m]$	Set ([10, 12, 14])
Turgor pressure of fresh cell (P_T)	200 $[kPa]$	[17]
Osmotic potential of fresh cell ($-\pi$)	$-$ 200 $[kPa]$	Equal to - P_T ([10, 14])
Cell fluid compression modulus(K)	20 $[MPa]$	Set ([10])
Number of fluid particles	1624	Set
Number of wall particles	1091	Set

Results and Discussion

In Fig. 4, the model predictions for the inflated turgid cell have been visualised and presented. It should be noted here that only the inflation stage of the cells have been considered in this stage. The mass transfer characteristics of the system will influence the inflation process (during inflation) and the shrinkage (during drying) in analogous ways as the same mass transfer characteristics and equation of state are involved in both the scenarios along with other formulae. At the same time, the way of assigning the end values of turgor pressure and osmotic potential are similar in the two cases. These are the critical factors which govern the shrinkage behaviour of the cell during either inflation

or shrinkage. Therefore it could be cogently suggested that it is possible to extrapolate the results for drying stages of the model by looking at results at the inflation stage. Accordingly, the cell fluid mass variation with the simulation time was observed and plotted for the each L_P value under consideration (see Fig. 5). It should be mentioned here that for very high (relatively) values of L_P (i.e. $\geq 2.5 \times 10^{-4}$ $m^2N^{-1}s$), the fluid mass variation could not be observed as the model became unstable during the simulations. In terms of numerical modelling, this means that the corresponding value is not favourable for the model under consideration and could be regarded as an unstable value under the given circumstances.

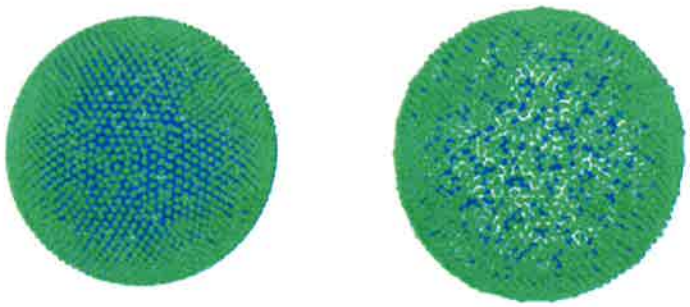

(a) (b)

Fig. 4. Visualisation of the model predictions for an inflated cell (a) fresh cell (b) inflated cell at fully turgid steady state conditions

According to the results, it could be deduced that L_P values of 2.5×10^{-5} $m^2N^{-1}s$ and 2.5×10^{-6} $m^2N^{-1}s$ lead to higher mass transfer rates and eventually higher fluid mass increments as shown in the graph in Fig. 5. The values of L_P below that (i.e. $\leq 2.5 \times 10^{-7}$ $m^2N^{-1}s$) lead to relatively very low mass transfer rates and eventually low fluid mass increments. Therefore such values could not be considered as favourable because they lead to higher computational times for achieving a given amount of fluid mass increment (similarly fluid mass losses in a drying situation). Therefore the values of 2.5×10^{-5} $m^2N^{-1}s$ and 2.5×10^{-6} $m^2N^{-1}s$ could be regarded as highly favourable as they lead to good computational efficiencies while maintaining a good stability in the model. Moreover, an L_P value of 2.5×10^{-5} $m^2N^{-1}s$ would be more favourable in terms of computational time as it leads to a lesser computational time than 2.5×10^{-6} $m^2N^{-1}s$. Further simulations will be necessary to test the stability of the model, since the curve related to L_P value of 2.5×10^{-5} $m^2N^{-1}s$ shows tendencies of instability (local maxima and minima) in Fig. 5.

During the drying operation of a plant tissue, the key driving forces are moisture content and the temperature. Moisture content has a strong correlation with the cell turgor pressure and temperature is similarly related to the relative humidity. Further, the drying temperature has a direct influence on the final nutritional value of a dried crop. A major deficiency in almost all recently reported meshfree-based numerical model on tissue scale drying phenomena is not being able to describe the influence of temperature and relative humidity. Incorporating temperature/humidity and related effects is an area for improvement in the field. Such a study is timely important as there is an exponentially growing attention in the current market towards the nutritional value of fruits as well as vegetables. Hence, a pivotal future work of this current study is to incorporate the temperature and humidity as two more governing parameters followed by the validation against experimental findings.

Acknowledgements

The authors of this study acknowledge the High Performance Computing (HPC) facilities of Queensland University of Technology (QUT), Brisbane, Australia; the financial support provided by

the CPME scholarship provided by the Science and Engineering Faculty (SEF), QUT; and the first author specifically extends the sincere support provided by University of Moratuwa, Sri Lanka.

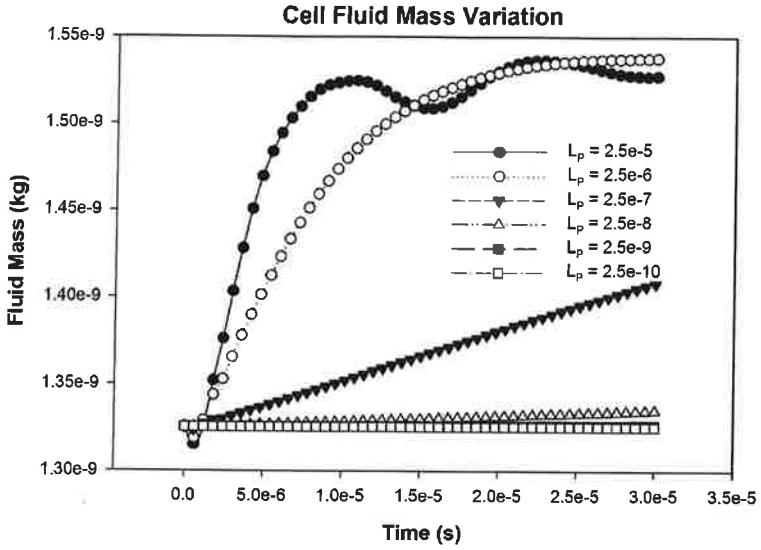

Fig. 5. Cell fluid mass variation with simulation time for different cell wall permeability (L_P) values

References

1. Jangam, S.V., *An overview of recent developments and some R&D challenges related to drying of foods.* Drying Technology, 2011. **29**(12): p. 1343-1357.
2. Stefan, G., S.R. Hosahalli, and M. Michele, *Drying of Fruits, Vegetables, and Spices*, in *Handbook of Postharvest Technology*. 2003, CRC Press. p. 653-695.
3. Mayor, L., M. Silva, and A. Sereno, *Microstructural changes during drying of apple slices.* Drying technology, 2005. **23**(9-11): p. 2261-2276.
4. Ramos, I.N., et al., *Quantification of microstructural changes during first stage air drying of grape tissue.* Journal of Food Engineering, 2004. **62**(2): p. 159-164.
5. Hills, B.P. and B. Remigereau, *NMR studies of changes in subcellular water compartmentation in parenchyma apple tissue during drying and freezing.* International journal of food science & technology, 1997. **32**(1): p. 51-61.
6. Lewicki, P.P. and G. Pawlak, *Effect of Drying on Microstructure of Plant Tissue.* Drying Technology, 2003. **21**(4): p. 657-683.
7. Bartlett, M.K., C. Scoffoni, and L. Sack, *The determinants of leaf turgor loss point and prediction of drought tolerance of species and biomes: a global meta-analysis.* Ecology Letters, 2012. **15**(5): p. 393-405.
8. Crapiste, G.H., S. Whitaker, and E. Rotstein, *Drying of cellular material—I. A mass transfer theory.* Chemical Engineering Science, 1988. **43**(11): p. 2919-2928.
9. Karathanos, V., G. Villalobos, and G. Saravacos, *Comparison of two methods of estimation of the effective moisture diffusivity from drying data.* Journal of Food Science, 1990. **55**(1): p. 218-223.
10. Karunasena, H.C.P., et al., *A coupled SPH-DEM model for micro-scale structural deformations of plant cells during drying.* Applied Mathematical Modelling, 2014. **38**(15–16): p. 3781-3801.
11. Nilsson, S.B., C.H. Hertz, and S. Falk, *On the Relation between Turgor Pressure and Tissue Rigidity. II.* Physiologia Plantarum, 1958. **11**(4): p. 818-837.
12. Liu, G.-R. and M. Liu, *Smoothed particle hydrodynamics: a meshfree particle method*. 2003: World Scientific.
13. Van Liedekerke, P., et al., *Particle-based model to simulate the micromechanics of biological cells.* Physical Review E, 2010. **81**(6): p. 061906.
14. Van Liedekerke, P., et al., *A particle-based model to simulate the micromechanics of single-plant parenchyma cells and aggregates.* Physical biology, 2010. 7(2): p. 026006.
15. Van Liedekerke, P., et al., *Mechanisms of soft cellular tissue bruising. A particle based simulation approach.* Soft Matter, 2011. 7(7): p. 3580-3591.
16. Wu, N. and M.J. Pitts, *Development and validation of a finite element model of an apple fruit cell.* Postharvest Biology and Technology, 1999. **16**(1): p. 1-8.
17. Wang, C., L. Wang, and C. Thomas, *Modelling the mechanical properties of single suspension-cultured tomato cells.* Annals of Botany, 2004. **93**(4): p. 443-453.